# The Transmission Function of Helium, Carbon and Iron and their flux inside the magnetosphere

Pavol Bobik*, Giuliano Boella†‡, Matteo J. Boschini†§, Massimo Gervasi†‡,
Davide Grandi†, Karel Kudela*, Simonetta Pensotti†‡, and Piergiorgio Rancoita†
*Inst. Exp. Physics, Dept. Space Physics, Slovak Academy of Sciences, Kosice (Slovak Republic)
†INFN Milano-Bicocca, Piazza della Scienza 3, 20126 - Milano (Italy)
‡Department of Physics, University of Milano-Bicocca, Milano (Italy)
§Cilea, Segrate - Milano (Italy)

***Abstract*— By using the trajectory calculations of Cosmic Rays (CR) inside the magnetosphere we have defined a Transmission Function (TF) to evaluate the particle flux approaching the Earth surface and the orbiting satellites. We used the IGRF and the Tsyganenko-96 models of the geomagnetic field and applied the backtracing method to obtain allowed and forbidden trajectories, in particular around the penumbra region of rigidity. We have computed the TF for Helium, Carbon and Iron, and compared the results with protons for different geomagnetic regions. We have also evaluated the flux of primary CR inside the magnetosphere and compared the results with the available measured data.**

## I. Introduction

### A. The Cosmic abundance

Galactic Cosmic Rays (GCR) are the dominant component of the charged particles present in space above few hundreds MeV of kinetic energy. Among them protons are largely the most abundant, but also the amount of Helium nuclei and electrons is relevant. In addition the presence of heavier nucleons, like Carbon, Nitrogen, Oxygen and Iron, is not negligible, in particular taking into account the amount of energy they can deposit.

It is important to evaluate both the absolute and relative abundance of the several components of the Cosmic Rays in relation to the radiation damage and radiation dose in space. The effect of radiation both on electronics stuff and organic tissue is depending on the absolute rate of CR, but it is related also to the relative abundance of ions (see [1], [2], [3], [4]). An accurate evaluation of these effects is even more important for long duration space missions, as it can be an interplanetary journey or for a permanent orbiting station like the International Space Station (ISS). An accurate evaluation of the radiation and its effect is unavoidable in particular for the manned missions.

Current estimates of cosmic abundances are based on measurements performed by several satellites, most of them operating outside the magnetosphere, and by stratospheric balloons (inside the magnetosphere) during the last 30-40 years. Due to the different experimental apparatus, to the long time interval, and to the different places and conditions, the several measurements can not represent a uniform sample. In order to perform a comparison we have decided to limit our analysis only to a couple of experiments, which have collected data in a similar condition.

### B. The Data sets

We have considered the data of protons and Helium from the AMS-01 detector, while the data of Carbon and Iron from the HEAO-3-C2 experiment. AMS-01 has collected data in June 1998 on board of the Space shuttle Discovery (flight STS-91) at an altitude of $\sim 380$ km, using a large collecting area ($\sim 1$ m$^2$) [5]. Its orbit had an inclination of 51.7 deg from the equatorial plane; the angular acceptance was a cone large $\sim 32$ deg from the detector axis, which was aimed, in most of the time of data taking, at the local zenith. During the 5-6 days of data taking, AMS-01 has detected $\sim 10^7$ protons in the range of kinetic energy $0.3 < E_k < 200$ GeV, and $\sim 10^6$ $\alpha$ particles in the energy range $0.1 < E_k < 100$ GeV/nucleon.

The HEAO-3-C2 experiment, on board of the HEAO-3 satellite, has measured the isotopic composition of the most abundant components of the CR flux with atomic mass between $A = 7$ and $A = 56$ and the flux of the several nucleons with charge between $Z = 4$ and $Z = 50$ [6]. HEAO-3 has been launched in September 1979; its altitude was $\sim 500$ km; the inclination of the orbit was $\sim 43.6$ deg from the equatorial plane; the angular acceptance of the detector HEAO-3-C2 was large $\sim 28$ deg from the axis, which was spinning around an axis pointing in direction of the Sun. We are using data of Carbon and Iron taken by HEAO-3-C2 experiment in the range of kinetic energy $0.6 < E_k < 35$ GeV/nucleon, during the time period from October 1979 to June 1980.

Data have been collected by the two detectors during periods of similar solar activity and polarity. HEAO has operated during 1980, at the beginning of the solar cycle 21, a period going from the minimum to the subsequent maximum of the solar activity with a positive solar magnetic field polarity ($A > 0$); AMS-01 was in orbit in June 1998, at the beginning of the solar cycle 23, again between the minimum and the subsequent maximum and with $A > 0$. The experimental conditions are also comparable: altitude and inclination of the orbit, angular acceptance of the detectors. The differential energy spectrum of protons, Helium, Carbon, and Iron, as measured by these experiments is shown in figure 1.

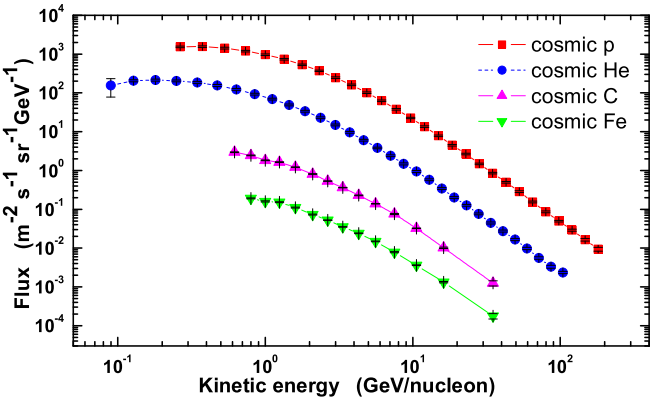


Fig. 1. Differential Cosmic Flux of p, He, C, Fe.

### C. The effect of Magnetosphere

In the space region around the Earth the Geomagnetic field provides a shield against the penetration of CR down to the Earth surface. To describe the effect of magnetic fields on charged particles we can introduce the magnetic rigidity $P$, essentially the ratio between the momentum of the particle ($p$) and its charge ($Zq$): $P = pc/Zq$, where $c$ is the speed of light. In this way we can define for every point in the space a limit called rigidity cut-off $P_{cut}$ (see [7], [8]). Below this limit primary CR will never reach the Earth surface or any detector in orbit. The value of the rigidity cut-off is position dependent, as it is larger in sites at lower geomagnetic latitude. Besides, all the nuclei are positively charged, therefore due to the charge drift some incoming directions are preferred (this effect is the origin of the East-West anisotropy).

## II. Calculation

### A. Description of the Magnetosphere

Trajectories calculations in the geomagnetic field are usually performed to estimate the particles approaching to a ground station or an orbiting satellite. The reconstruction of the particle trajectory is necessary to study the properties of CR inside the magnetosphere and to understand their nature, especially in the so called penumbra region, the region around the rigidity cut-off, whose definition is still empirical. This study can be done by using a software code reproducing the interaction between a charged particle and all the magnetic fields along the whole path.

The magnetic field close to the Earth surface is at first approximation a dipole, but moving away from the Earth other contributes become important. Among these we can mention: the several currents (ring current, Birkeland currents and tail currents) due to charged particles trapped inside the magnetosphere, the effect of the reconnection of the interplanetary magnetic field (few nT) and the geomagnetic field at the magnetopause. Moreover the latitudinal dependence is not geographically symmetric, because the Earth magnetic dipole is both tilted and shifted. This means that the geomagnetic equator is located in a tilted surface in the space, slowly moving in time in relation to the magnetic poles location. Due to all these features the story of a charged particle moving in the magnetosphere is not so easily predictable.

We have developed a code to reconstruct the Cosmic Rays trajectory in the Earth magnetosphere (see [9], [10]). This code solves the Lorentz equation and propagates a particle backward in time. The total magnetic field is evaluated by using the International Geomagnetic Reference Field (IGRF) 2000-2005 [11], representing the main contribution due to the inner Earth, and the external magnetic field Tsyganenko-96 (see [12], [13]), representing all the other contributions, like particle currents in the magnetosphere.

The code is time dependent: it must take into account both the long term variation (running over years) of the inner Earth magnetic field and the short term variation (changing in few days) of the external field. Besides most of the long term variation is related to the solar activity through the solar wind effect and its interaction with the Earth magnetic field and through the modulation of the GCR in the solar cavity.

The Earth magnetopause is calculated using the Sibeck equation [14] modified by Tsyganenko [12] for the solar wind effect. We have introduced an empirical magnetosphere boundary large 25 Earth radii in the night-side region to avoid long calculations in the far tail. Access for primary cosmic ray to some place is supposed to be allowed when the back-traced particle trajectory reaches the magnetopause or the magnetospheric boundary. As internal boundary we have considered a sphere at an altitude of 40 km, corresponding to the surface containing the $99\%$ of the Earth atmosphere.

### B. Transmission Function

Charged particles (protons and nucleons) are generated by the tracing code at a fixed altitude, in particular at the position of the space detectors AMS-01 and HEAO-3. They are back-traced in time until they reach one of the two boundaries: the magnetopause/magnetosphere boundary or the atmosphere. In the first case the particles are considered to be primary CR, otherwise secondary CR. The external field is evaluated taking into account the parameters changing with the solar activity. Those parameters are evaluated at the time of the data taking of the two experiments.

The TF has been calculated in the following way: for every position $i_M$ in a certain geomagnetic region **M**, for a fixed rigidity $P$, we have evaluated the ratio $R^{i_M} = N^{i_M}_{all}/N^{i_M}_{total}$ between the number of allowed trajectories $N^{i_M}_{all}$ and the number of all the computed trajectories $N^{i_M}_{total} = N^{i_M}_{all} + N^{i_M}_{forb}$. This ratio represents the probability for particles with rigidity $P$ to reach this geographic position coming from outside the magnetosphere. Then, for every geomagnetic region **M**, we have averaged the ratio $R^{i_M}$ over all the positions $i_M$. This average ratio $TF_M(P) = \langle R^{i_M} \rangle$ represents the transmission function for a particle with rigidity $P$ to reach that geomagnetic region **M**, at the altitude of AMS or HEAO-3. This is indeed a very wide region with a complex structure of penumbra changing from position to position. We have selected a grid of 3600 positions and from every point we have generated particles in

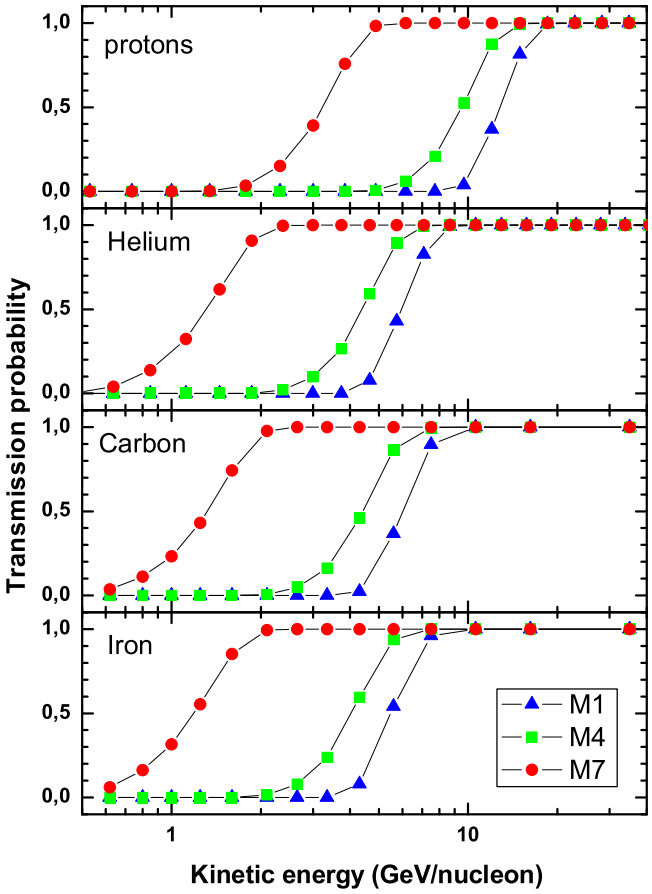


Fig. 2. Transmission Function of p, He, C and Fe, in the geomagnetic regions **M1**, **M4**, **M7**.

1800 directions outwards. Each starting position and direction has been chosen in order to have a uniformly distributed sample.

We have considered the AMS geomagnetic regions (see [5], [10]), defined as a function of the geomagnetic latitude, from **M1**, around the magnetic equator, to **M10**, near the magnetic poles. For that regions we have computed the transmission function $TF_M(P)$. In every region **M** a particle with a rigidity ($P$) lower than a threshold value (usually called rigidity cut-off, $P_{cut}$) can not enter the magnetosphere. For $P << P_{cut}$ we obtain $TF_M = 0$, while for $P >> P_{cut}$ we have $TF_M = 1$. This threshold value is decreasing going towards the magnetic poles, but is nearly independent from the nucleon considered.

Besides, looking at the $TF_M$ in terms of kinetic energy, instead of rigidity, we can find a shift in the cut-off region for the nuclei respect to protons. This effect arises because the ratio $Z/A \simeq 1/2$ for almost all the nuclei (like He, C and Fe) except the H (protons) for which the ratio $Z/A \simeq 1$. This effect can be observed in the figure 2, where $TF_M$ is shown for the regions **M1**, **M4**, **M7**, as a function of the kinetic energy.

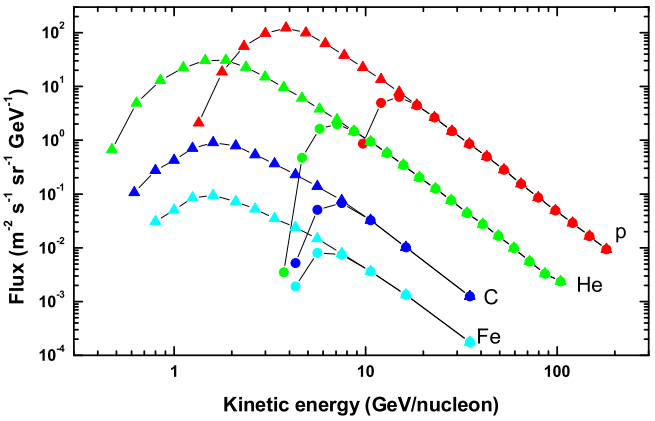


Fig. 3. Flux of primaries p, He, C and Fe, in the geomagnetic regions **M1** (circles), and **M7** (triangles).

## III. Results

### A. Flux inside the magnetosphere

We have computed the flux of primary CR entering each geomagnetic region **M**. Using the $TF$ calculated, as described above, we obtain the component of primary CR from the AMS-01 cosmic flux for p and He and from HEAO-3-C2 flux for C and Fe, as shown in figure 1. We call $TF_M(E_i)$ the Transmission Function relative to the energy bin $i^{th}$ and we obtain the primary flux $\Phi_M^{pri}(E_i)$ in the region **M**, using the Cosmic flux $\Phi^{cos}(E_i)$:

$$\Phi_M^{pri}(E_i) = \Phi^{cos}(E_i) \cdot TF_M(E_i) \qquad (1)$$

In figure 3 we present the flux of p, He, C, and Fe for the geomagnetic regions **M1** (higher value of the energy cut-off) and **M7** (lower value of the energy cut-off). As for the Transmission Function, the cut-off in the same geomagnetic region occurs at the same value of rigidity, but at different values of kinetic energy, as shown in figure 3.

### B. Relative abundances

In order to evaluate the relative abundance of He, C and Fe, respect to the protons, inside the several geomagnetic regions, the integral flux above a certain value of kinetic energy has been computed. In fact inside the magnetosphere all the particles above the local rigidity cut-off are present and contribute to the dangerous radiation. Therefore the relative abundance has been defined as the ratio $\Re$ of the integral flux of Helium, Carbon, Iron, respect to the flux of protons. We have computed $\Re$ using the primary flux $\Phi^{pri}$ integrated above the quoted value of kinetic energy ($E$) [15]:

$$\Re_{He/p}(E) = \frac{\int_E^\infty \Phi_{He}^{pri}(E')\ dE'}{\int_E^\infty \Phi_p^{pri}(E')\ dE'} \qquad (2)$$

$$\Re_{C/p}(E) = \frac{\int_E^\infty \Phi_C^{pri}(E')\ dE'}{\int_E^\infty \Phi_p^{pri}(E')\ dE'} \qquad (3)$$

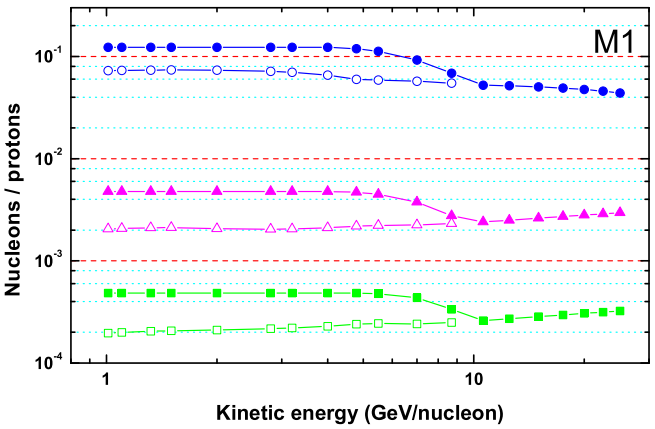


Fig. 4. Abundance of primary He (solid circles), C (solid triangles) and Fe (solid squares) nucleons respect to the protons, in the geomagnetic region **M1**. For comparison the cosmic abundance of He (open circles), C (open triangles) and Fe (open squares) nucleons is also shown. The abundances are defined as the ratio $\Re$ of the fluxes integrated above the quoted energy (see the text for more details).

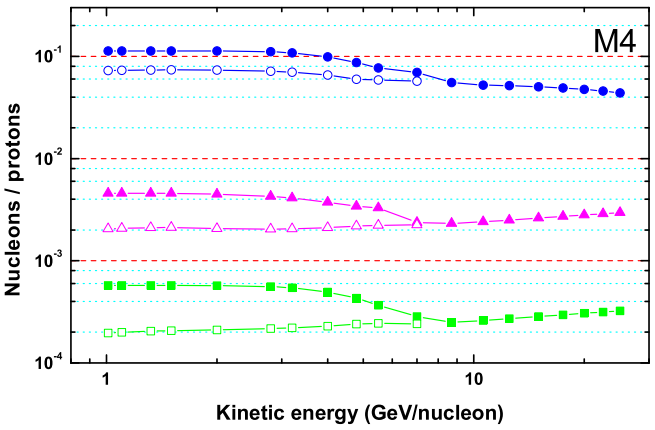


Fig. 5. Abundance of primary He, C and Fe nucleons respect to the protons, in the geomagnetic region **M4**. The meaning of the used symbols is described in the caption of figure 4.

$$\Re_{Fe/p}(E) = \frac{\int_E^\infty \Phi_{Fe}^{pri}(E')\ dE'}{\int_E^\infty \Phi_p^{pri}(E')\ dE'} \qquad (4)$$

In this calculation the contribution of the modelled high energy tail is negligible ($< 1\%$): only the highest energy value could be affected. Ratios $\Re$ for the regions **M1**, **M4**, and **M7** are shown respectively in the figures 4, 5, and 6. The limit at high energy is equal to the ratio $\Re$ as measured outside the magnetosphere: the cosmic abundance $\Re^{cos}$. On the other hand the limit at low energy is the ratio ($\Re^M$) as obtained considering all the particles penetrated inside the magnetosphere in that geomagnetic region. The transition between the two regimes occurs around the rigidity cut-off and it changes with the geomagnetic region.

In the figures 4, 5, and 6, the cosmic ratio $\Re^{cos}$ extended below the rigidity cut-off is also shown (open symbols), in agreement with figure 1, for comparison with the abundace

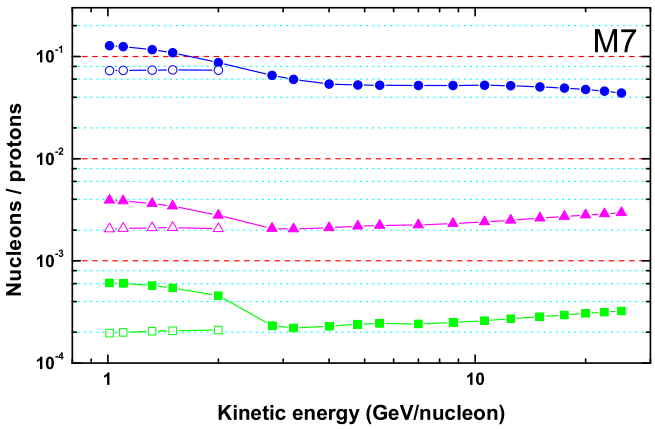


Fig. 6. Abundance of primary He, C and Fe nucleons respect to the protons, in the geomagnetic region **M7**. The meaning of the used symbols is described in the caption of figure 4.

observed inside the geomagnetic regions (solid symbols). It is clear as below the cut-off the abundance inside the magnetosphere is larger than the cosmic one. This effect is due mainly to the different energy cut-off obtained for the nucleons, respect to the protons. As shown in figure 3 the energy cut-off for nucleons is shifted by a factor of $2-3$ towards lower values.

The cosmic ratio $\Re^{cos}$, as shown in the figures, for all the three nucleons is not constant with energy. This is because the spectra have a slightly different power law. This difference in the steepness can be only partly real, because the uncertainties in flux measurement could be important, especially for C and Fe. In any case in the considered range of energy the variation of $\Re^{cos}$ is less than a factor 2.

### *C. Discussion*

The average value of the abundance, in the two limits, $\Re^{cos}$ at high energy and $\Re^M$ at low energy, is also indicated in Table I for He, C, and Fe. In order to evaluate the abundance enhancement (Æ) inside the magnetosphere we need to compare the value $\Re^M$ and $\Re^{cos}$ at a kinetic energy ($E_{æ}^M$) which is just lower than the value of the kinetic energy corresponding to the local geomagnetic cut-off ($E_{cut}^M$):

$$Æ^M = \frac{\Re^M(E_{æ}^M)}{\Re^{cos}(E_{æ}^M)} \qquad (5)$$

In fact at this effective energy ($E_{æ}^M$) the differential primary fluxes are null and the ratio $\Re^M$ is computed using the whole population of nucleons and protons. The abundance enhancement $Æ^M$ is also shown in Table I, together with the effective energy ($E_{æ}^M$) where it has been evaluated, for the several geomagnetic regions. The enhancement values range from 1.5 for He/p ratio in the region **M4** to 3.1 for Fe/p ratio in the region **M7**. Most of the increment values are $\sim 2$.

As discussed above, the cut-off of the fluxes is directly related to the rigidity of the charged particle in the geomagnetic region considered. For this reason we can compare the ratio

TABLE I

ABUNDANCE RATIO OF HE/P, C/P AND FE/P EVALUATED BOTH BELOW AND ABOVE THE ENERGY CUT-OFF, FOR THE GEOMAGNETIC REGIONS M1, M4 AND M7. THE ABUNDANCE ENHANCEMENT Æ AND ITS RELATIVE ENERGY $E_{æ}^{M}$ IS ALSO SHOWN (SEE THE TEXT FOR MORE DETAILS).

| | $\Re_{He/p}^{M}$ | $\Re_{He/p}^{cos}$ | $Æ_{He/p}$ | $E_{æ}^{M}$ (GeV) |
|---|---|---|---|---|
| M1 | $1.2 \cdot 10^{-1}$ | $4.4 - 5.1 \cdot 10^{-2}$ | 1.9 | $3 - 4$ |
| M4 | $1.1 \cdot 10^{-1}$ | $4.4 - 5.2 \cdot 10^{-2}$ | 1.5 | $1.5 - 2.0$ |
| M7 | $1.2 \cdot 10^{-1}$ | $4.4 - 5.8 \cdot 10^{-2}$ | 1.7 | $1.0 - 1.2$ |
| | $\Re_{C/p}^{M}$ | $\Re_{C/p}^{cos}$ | $Æ_{C/p}$ | $E_{æ}^{M}$ (GeV) |
| M1 | $4.5 \cdot 10^{-3}$ | $2.5 - 2.8 \cdot 10^{-3}$ | 2.3 | $3 - 4$ |
| M4 | $4.5 \cdot 10^{-3}$ | $2.4 - 2.8 \cdot 10^{-3}$ | 2.2 | $1.5 - 2.0$ |
| M7 | $4.0 \cdot 10^{-3}$ | $2.2 - 2.8 \cdot 10^{-3}$ | 1.9 | $1.0 - 1.2$ |
| | $\Re_{Fe/p}^{M}$ | $\Re_{Fe/p}^{cos}$ | $Æ_{Fe/p}$ | $E_{æ}^{M}$ (GeV) |
| M1 | $5.0 \cdot 10^{-4}$ | $2.6 - 3.0 \cdot 10^{-4}$ | 2.0 | $3 - 4$ |
| M4 | $5.7 \cdot 10^{-4}$ | $2.5 - 3.0 \cdot 10^{-4}$ | 2.8 | $1.5 - 2.0$ |
| M7 | $6.0 \cdot 10^{-4}$ | $2.4 - 3.0 \cdot 10^{-4}$ | 3.1 | $1.0 - 1.2$ |

TABLE II

COSMIC ABUNDANCE RATIO OF HE/P, C/P AND FE/P AS A FUNCTION OF THE RIGIDITY EVALUATED IN THE RANGE OF VALUES CORRESPONDING TO THE KINETIC ENERGY BELOW CUT-OFF, FOR THE GEOMAGNETIC REGIONS M1, M4 AND M7 (SEE THE TEXT FOR MORE DETAILS).

| | $\Re^{cos}(P)$ | $P$ (GV) |
|---|---|---|
| He/p | $1.1 - 1.5 \cdot 10^{-1}$ | $2 - 10$ |
| C/p | $3 - 5 \cdot 10^{-3}$ | $2 - 10$ |
| Fe/p | $4 - 6 \cdot 10^{-4}$ | $2 - 10$ |

$\Re^{M}$ with the cosmic abundance evaluated as a function of the rigidity $P$. We have to evaluate $\Re^{cos}(P)$ at a rigidity comparable to the kinetic energy $E_{æ}^{M}$ (see Table II). As shown in Tables I and II, the values $\Re^{M}$ we find at low energy are comparable to the relative abundances evaluated in rigidity ($\Re^{cos}(P)$). This means that the abundance ratio $\Re$ inside the magnetosphere can be also evaluated by using the ratio $\Re^{cos}(P)$ evaluated below the rigidity cut-off of the geomagnetic region considered.

## IV. CONCLUSIONS

We have used a tracing code to define a transmission function for the CR penetrating inside the magnetosphere. In this way we have computed the transmission probability for protons, Helium, Carbon and Iron nuclei inside several geomagnetic regions. Combining the TF with the cosmic flux we are able to obtain the primary CR flux inside the magnetosphere for the several geomagnetic regions. These primary CR fluxes result truncated, as expected, at energy lower than the local effective cut-off.

While the rigidity cut-off occurs at the same value for the different nuclei, inside the same geomagnetic region, the cut-off in terms of kinetic energy is changing. This effect is driven by the different ratio between elementary charges ($Z$) and atomic mass units ($A$). The effect is particularly important when protons, for which we have $Z/A \simeq 1$, are compared with other nuclei like Helim, Carbon and Iron, for which we obtain $Z/A \simeq 1/2$.

Therefore inside the magnetosphere we need to consider the ions abundance, respect to the protons, taking into account the rigidity selection. The abundance of the several nuclei inside the magnetosphere are then compared with the cosmic abundance, which take into account the flux outside the magnetosphere. We have found that the ions flux ratio inside the magnetosphere is larger than the cosmic flux ratio by a factor $\sim 1.5 - 3$. Finally this magnetospheric abundances are comparable with the abundance ratios obtained using fuxes evaluated in rigidity.

These results must be considered when the effects of radiation on orbiting satellites are evaluated. In fact the effect of radiation damage depends both on the absolute flux of CR and on the relative abundance of the different nuclei.

## REFERENCES


[1] C. Consolandi et al., *NIM B*, in press, *doi:10.1016/j.nimb.2006.08.018* (2006).
[2] D. Codegoni et al., *Nucl. Instr. and Meth. in Phys. Res.* **B 217**, 65 (2004).
[3] A. Colder et al., *Proc. of the* $7^{th}$ *ICPPAT*, Como 15-19 October 2001, World Scientific (Singapore) 780 (2002).
[4] A. Colder et al., *Proc. of the European Space Component Conference* (Toulouse 24-27 September 2002), ESA **SP-507**, 377 (2002).
[5] AMS collaboration - M. Aguilar et al., *Phys. Rep.*, **366**, 331 (2002).
[6] J.J. Engelmann et al., *Astron. & Astrophys.*, **233**, 96 (1990).
[7] K. Stoermer, *Z. Astroph.*, **1**, 237 (1930).
[8] E. Fermi, *Nuclear Physics*, The University Of Chicago press (1950).
[9] P. Bobik et al., *AGU Geophysical Monograph Series*, **155**, 301 (2005).
[10] P. Bobik et al., *J. Geophys. Res.*, **111**, A05205 (2006).
[11] Barton, C.E., International Geomagnetic Reference Field: The Seventh Generation, *J. Geomag. Geoelectr.*, **49**, 123 (1997).
[12] N.A. Tsyganenko, *J. Geophys. Res.*, **100**, 5599 (1995).
[13] N.A. Tsyganenko, and D.P. Stern, *J. Geophys. Res.*, **101**, 27187 (1996).
[14] D.G. Sibeck et al., *J. Geophys. Res.*, **96**, 5489 (1991).
[15] P. Bobik et al., Proc. of 9th Conf. Astroparticle, Particle and Space Physics, Detectors and Medical Physics Applications, *World Scientific Publishing*, 928 (2006).